The Dynamic Crystallization and Multiple Melting Behavior of Polypropylene in the In-Reactor Alloy: A Differential Scanning Calorimetry Study

Haijin Zhu, Hengrui Yang, Ying Zhao, Dujin Wang

Beijing National Laboratory for Molecular Sciences, CAS Key Laboratory of Engineering Plastics, Institute of Chemistry, Chinese Academy of Sciences, Beijing 100080, China

ABSTRACT: The isothermal and nonisothermal crystallization and the subsequent melting behaviors of the polypropylene (PP) component in the in-reactor alloy were studied systematically by a series of thermal analysis techniques. The alloy sample used in the present study is a newly invented *in situ* blend of polypropylene with high ethylene–propylene rubber content. The effect of annealing temperatures on the subsequent crystallization and melting process of PP was explained by the different molecular behavior in the three "temperature domains." Multiple melting endotherms were also observed for the nonisothermally crystallized sample, and were attributed to the dynamic melting process which consists of three steps: melting, recrystallization, and remelting. The melting temperature of initial mesomorphic phase is found to be very close to the temperature of recrystallization or reorganization. To separate the recrystallization process from the overlapping processes, the difference spectra of fast and slow heated DSC endotherms were used, which is based on a straight forward but reasonable assumption. In addition, temperature modulated differential scanning calorimetry (TMDSC) has also been used to study the melting of PP component. © 2011 Wiley Periodicals, Inc. J Appl Polym Sci 121: 1372–1383, 2011

Key words: polypropylene; in-reactor alloy; multiple melting; DSC

INTRODUCTION

Polypropylene (PP) has been widely used in the industries because of its excellent mechanical properties, improved processability, and relatively low cost. However, the poor low temperature impact strength significantly limits its applications, e.g., in automobile parts, appliance, and other industry uses. To improve its impact behavior, PP is usually toughened by the addition of various rubbers, such as ethylene–propylene rubber (EPR),[1,2] propylene-1-hexene copolymers,[3] and ethylene-1-butylene copolymers.[4] Among the ways of toughening PP, the "Reactor Granule Technology (RGT)" has been proved to be efficient in improving the inherently poor impact properties of polypropylene.[5] The PP in-reactor alloy produced via RGT is superior to mechanical blends in both the mechanical properties and the product cost. Moreover, the polymer chain structure and the overall composition of the in-reactor alloy can be precisely controlled over a wide range. An in-reactor alloy system generally shows very complicated microstructures and typically heterophasic morphology, which consists of ethylene-propylene random copolymer, ethylene-propylene segmented copolymers with different sequence lengths of polyethylene (PE) and polypropylene (PP) segments, and homo polypropylene (HPP).[6,7]

It is understandable that the mechanical properties of PP in-reactor alloy are related to both the microphase-structure of the blend system and the crystallization behavior of each component. However, most of previous studies, if not all, mainly focus on the phase structure and the composition of the alloy, and try to correlate them with either the polymerization mechanisms or the mechanical properties of the material.[1,2,8–13] The crystallization and melting behavior of PP in the in-reactor alloy has been seldom reported.

There has been a lot of research on the melting behavior of pure isotactic polypropylene (iPP), especially on the origin of its multiple melting peaks.[14–18] A numbers of explanations have been proposed

for the multiple melting characteristics. In 1960s, Kawai firstly considered it a kind of molecular fractionation during isothermal crystallization process.[19] Kamide and Yamaguchi investigated the isothermal crystallization behavior of iPP with different molecular weight distribution and concluded that the molecular weight fractionation mechanism does not play an important role during isothermal crystallization process if the polymer does not have a very low molecular weight component.[18] Later on, the effect of lamellar thickening mechanism has been confirmed experimentally by Mezghani et al.[20] Kim et al. studied the multiple melting behavior of iPP by annealing the sample at different temperatures, and attributed the double peaks to the melting of two different preexisting crystals originating from molecules with different molecular weights.[21] Despite the controversy in the past, a general consensus has been achieved among most of the authors in the recent couple of years. The multiple melting behavior of iPP can be explained from two aspects. One is concluded from the morphological point of view, explaining that the appearance of two melting peaks can be attributed to two kinds of lamellae, crosshatched, and radiating dominant lamellae.[16,17,22] The other explanation is based on the thermal dynamic point of view, ascribing the multiple melting behavior to the recrystallization or reorganization of the imperfect lamellae.[15,23] Although recrystallization is a very common phenomenon in the melting process of polymers, there are seldom any solid evidences as it is an exothermic process and severely overlapped with other endothermic processes. Therefore, it is not easy to be identified by the routine analytical techniques. To separate the recrystallization process from the overlapping processes, a quite straight forward but efficient way was proposed, and temperature modulated differential scanning calorimetry (TMDSC) has also been applied in the study.

Although the melting behavior of iPP has been extensively studied, little is known about the PP in-reactor alloy. The crystallization and melting behavior of PP in the alloy should be different from that of the pure iPP because of the presence of block copolymer which are partially miscible with PP matrix and served as a compatibilizer between the PP matrix and dispersed rubber phase. In our previous publication in this series,[7] we have systematically studied the compositional heterogeneity and phase structure of the polypropylene in-reactor alloy. In this article, particular attention is served to the non-isothermal crystallization and the subsequent melting behavior of PP in the in-reactor alloy, trying to achieve a complete understanding of the thermal dynamic mechanism behind the crystallization and melting phenomenon.

EXPERIMENTAL

Materials

A commercial PP/ethylene–propylene in-reactor alloy was used, which was produced by Basell using a spherical superactive $TiCl_4/MgCl_2$-based catalyst. The composition of the alloy was characterized in our previous paper.[7] Three components have been identified from the combination of solution NMR, analytical TREF and SEM results: homo polypropylene (HPP), ethylene–propylene segmented copolymer with crystallizable ethylene and propylene blocks, and ethylene–propylene random (EPR) copolymer which is not crystallizable.

Differential scanning calorimetric analysis

A Mettler 822e differential scanning calorimetric (DSC) apparatus was used for the thermal analysis of the PP in-reactor alloy. About 2.5 mg of the sample was cut from the pellets and sealed in an aluminum pan. The calibration of the temperature scale and the heat flow was achieved from the melting scans of high-purity indium and zinc samples at the same heating rate. The heat history of the samples was eliminated by holding the temperature at 230°C for 5 min. Subsequently, the samples were cooled to 0°C and reheated to 210°C at different scanning rate. The crystallization and melting temperatures were determined by using the peak values of the corresponding thermograms. The small endotherm at ~ 120°C and exotherm at ~ 102°C are due to the melting and crystallization of PE and PE blocks in the segmented copolymers [Fig. 1(a,b)]. The endotherms above 130°C and exotherms above 110°C are ascribed to the melting and crystallization of iPP and iPP blocks in the segmented copolymers. For single-step self-nucleation and annealing experiments, heating and cooling rate of 10°C/min was used for all the scans.

Successive self-nucleation and annealing

Successive self-nucleation and annealing (SSA) is essentially a thermal fractionation method, which is based on the sequential application of self-nucleation and annealing steps on polymer samples.[24,25] The first self-seeding temperature (T_s), which is thought to be one of the most important parameters in SSA, was suggested by Mueller to be the minimum temperature within annealing temperature domain II, since this is the temperature that causes the maximum shift in crystallization temperature (T_c) without any annealing.[25] Therefore, the T_s of the PP component in the alloy, as determined by a series of single-step self-nucleation experiments, is 171°C. The SSA was performed according to the following
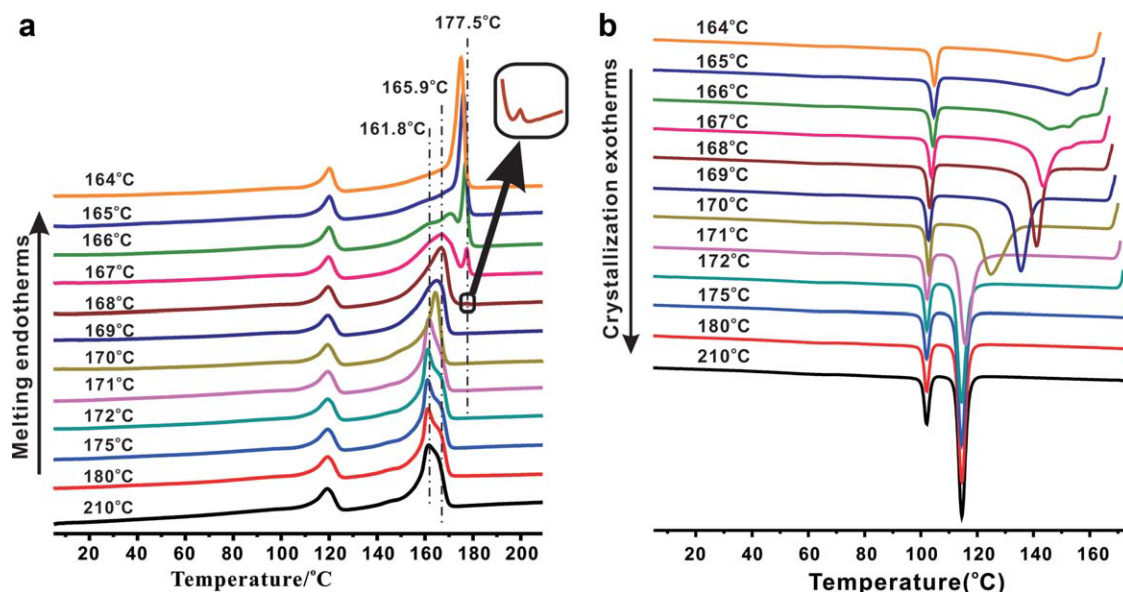
Figure 1 (a) DSC melting endotherms and (b) crystallization exotherms of the PP in-reactor alloy annealed at different temperatures. The annealing temperatures are indicated above the corresponding curves in the figures. [Color figure can be viewed in the online issue, which is available at wileyonlinelibrary.com.]

procedure. The sample was first heated to and held at 230°C for 5min under nitrogen atmosphere and then decreased to 0°C at a rate of 20°C/min to create a standard thermal history. The fraction window adopted here was 5°C, and the annealing time was 30 min. The scanning rate during the thermal conditioning steps was 20°C/min. Pijpers et al. introduced the high-speed calorimetry concept that the increment in heating rate can be compensated by reducing the sample mass.[26] Recently, this concept was introduced into the SSA protocol by Lorenzo to reduce the thermal fractionation time.[24] So, a higher scanning rate of 20°C/min (normally 10°C/min) was used during the thermal cycles, and a small sample mass of 2.4 mg (normally 4–5 mg) was used as compensation. After completion of the fractionation process, the melting endotherm was recorded at a heating rate of 10°C/min.

Temperature modulated differential scanning calorimetry

TMDSC measurement was performed in a DSC-Q100 from TA Instruments under modulated mode. The temperature amplitude of the modulation was 0.5°C, and the period was 40 s (frequency of 25 mHz). The underlying heating rate was 2°C/min.

XRD measurement

The X-ray diffraction patterns were recorded on a Rigaku D/max 2500 X-ray powder diffractometer using Cu Kα radiation (40 kV, 200 mA). The X-ray wavelength used was 0.154 nm; step of 0.02° and 2θ range of 5–30° were selected.

RESULTS AND DISCUSSION

Self-nucleation and annealing behavior of PP in-reactor alloy

Single-step self-nucleation and annealing

As mentioned in the introduction part, the PP in-reactor alloy consists of homo polypropylene (HPP), ethylene-propylene segmented copolymer with different PP and PE sequence length, as well as EPR copolymer. It is well known that HPP is a semicrystalline polymer with polymorphic crystalline modifications. Because of the incompatibility between the HPP and EPR component, the crystallization behavior of HPP in the bulk can hardly be influenced by the presence of EPR since they are phase separated in their blends. The ethylene–propylene segmented copolymer was, however, found to be partially miscible with HPP depending on the sequence of the polymer chain.[10] So, the overall crystalline morphology and crystallization kinetics of the HPP component in the alloy may be affected by the presence of E-P segmented copolymer. The melting and crystallization traces of PP in-reactor alloy annealed at different temperatures are shown in Figure 1(a,b), respectively. It can be seen that the effect of annealing temperature on the subsequent melting and crystallization behavior is quite similar. The melting and crystallization of PP component are not affected by the annealing temperature higher than 172°C. As the annealing temperature decreases from 171 to 169°C, the corresponding crystallization peaks of PP component get broader and shift to much higher temperature, whereas the subsequent melting temperature
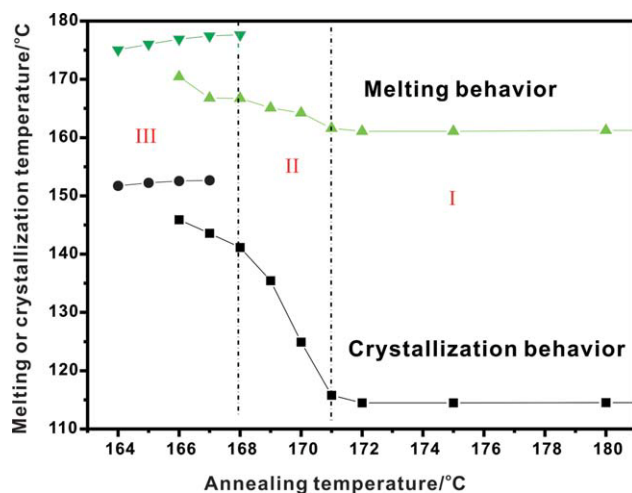
Figure 2 Effect of annealing temperature on the crystallization and subsequent melting behavior of PP component in PP in-reactor alloy. [Color figure can be viewed in the online issue, which is available at wileyonlinelibrary.com.]

does not change so significantly. Annealing the sample at temperature lower than 168°C produces a new crystalline species (a new crystalline peak can be identified) which melts at much higher temperature (177°C). It is also very interesting to notice that triple melting peak was found after been annealed at the temperature of 166°C. This phenomenon was also observed for the nonisothermal crystallized sample, and the origin will be discussed later in the corresponding section.

The melting and crystallization temperature obtained from the thermograms in Figure 1 are plotted as a function of annealing temperature in Figure 2. The whole melting or crystallization range of PP component in the alloy can be divided into three domains according to its different characteristic in the nucleation and lamellae thickening behavior during the annealing process.[27] In domain I (annealing temperature higher than 171°C), the system is completely melted, leaving only very small amount of ultra-high molecular weight molecules and other impurities (catalysis residues, etc.) in the system as nuclei. The melting and crystallization temperature are the same as compared to the standard process without annealing, indicating that a constant nucleation density was achieved in domain I. When annealed in domain II, the crystallization temperature shifts to much higher value while the subsequent melting does not reveal any traces of annealing, exhibiting a characteristic behavior of exclusive self-nucleation. This is because in domain II, the temperature is high enough to melt almost all of the polymer crystals, but low enough to leave "small" crystal fragments that can act as self-nuclei. These fragments are not really crystalline lamellae, but some ordered structure in the melt produced by melting of the crystalline structure. These

fragments are so small that they can't be annealed, and basically cannot cause lamellae thickening during the annealing process. Therefore, the melting temperature of the resulting lamellae formed in the subsequent cooling process does not differ very much from that of the unannealed sample. However, the presence of these "small" crystal fragments can act as nuclei and reduce the energy barrier remarkably during the crystallization process, this is the reason why the crystallization temperatures increase significantly after been annealed in domain II. When annealed in domain III, a portion of perfectly arranged lamellae with high melting point remain unmelted and can act as nuclei during annealing process. The mobile PP molecules thus fold on the surface of the unmelted lamellae and thicken it. The lamellae formed in the annealing process in domain III are more thick and regular than the lamellae formed during the subsequent cooling process, and thus tend to melt at higher temperature.

Successive self-nucleation and annealing

To further investigate the detailed melting behavior of the PP in-reactor alloy, and to correlate the melting behavior with the molecular architecture, SSA technique was used. SSA is essentially a thermal fractionation technique based on sequential application of self-nucleation and annealing steps on polymer samples. SSA fractionates the polymers mainly according to the distribution of defects (branches) on the polymer chain, whereas with a minor influence by the molecular weight distribution.[28,29] As been stated in the experimental section, besides the homo-polypropylene, some segmented ethylene–propylene copolymer with different sequence lengths also presents in the alloy. So, this segmented copolymer component is expected to be fractionated by the SSA procedure according to the polypropylene sequence length.

Figure 3 shows the DSC endotherms of the alloy after having been subjected to SSA treatments. A standard DSC thermogram with cooling rate of 20°C/min and heating rate of 10°C/min is also presented in the figure for comparison. A series of melting endotherms can be observed, indicating that thermal fractionation has occurred during the SSA treatment. The fractions that exhibit the highest melting points are those with the longest propylene segments incorporated within the specific lamellar population. The first two melting peaks (Peaks 1 and 2) are exceptionally separated from each other. The other peaks, however, are less resolved. Care must be taken to explain the origin of these two melting peaks as the normal SSA fractionation mechanism may not be suitable in this case. It is speculated that both the first two melting peaks are assigned to the melting of homo-polypropylene
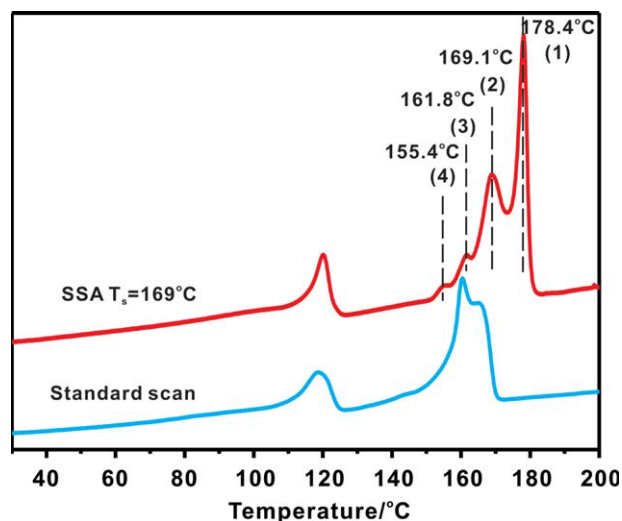
Figure 3 DSC melting endotherms of PP in-reactor alloy with and/or without SSA treatment. The first self-seeding temperature (T_s) of 169°C was determined by using the lowest temperature point in the annealing temperature domain II. The endotherm of the standard scan was used as a comparison. [Color figure can be viewed in the online issue, which is available at wileyonlinelibrary.com.]

component. These two peaks were not segregated by the molecular chain defects, but by the melting–recrystallization–remelting process during heating. Note that the two melting peaks present at higher temperature compared with the melting peak in the standard scan. Based on the above observations, Peak 1 is probably ascribed to the annealed HPP crystalline species, Peak 2 to the recrystallized HPP lamellae. Peaks 3 and 4, however, are originated from the melting of the ethylene–propylene segmented copolymers with different propylene sequence lengths, which were segregated during the SSA procedure.

As it has been stated previously, the SSA procedure fractionates the E-P segmented copolymer mainly by its compositional heterogeneity. Each endotherm represents a population of crystals with similar thermodynamic stability, and the normalized differential area under each endothermic peak is proportional to the mass of molten lamellae within the temperature interval. Peaks 2–4 are not very well resolved, because for one thing, the amount of E-P segmented copolymer with crystallizable propylene sequences is very small, and thus the melting enthalpy is small; for another, the melting peaks of segmented copolymer are overlapped with the melting endotherms of the imperfect HPP lamellae, which are prone to melt at lower temperature.

Effect of annealing time on the melting
behavior of PP in-reactor alloy

Three melting regions of iPP have been determined by isothermal crystallization experiments in the pre-

vious section. The aim of this experiment is to study the effect of annealing time on the subsequent melting behavior when the sample is annealed in region III. Figure 4 shows the DSC melting curves of the alloy annealed at 163°C for various time. The annealing temperature was selected to be the valley point between the two melting peaks. The sample was first cooled from 230°C to room temperature at a rate of 30°C/min, and then heated to the target temperature for annealing. The annealed sample was then cooled to room temperature. Finally, the exothermic curve of the thermal-treated sample was recorded with the heating rate of 5°C/min. It can be seen in Figure 4 that only a single sharp peak is observed and the lower enothermic peak presents as a shoulder after annealing. The intensity of the lower temperature shoulder decreases with the annealing time, whereas the intensity of the sharp peak at higher temperature increases. This may due to the fact that the imperfect lamellae formed during the fast cooling process gradually melted, and then rearranged and recrystallized at the annealing temperature (163°C). So, the amount of imperfect lamellae is reduced gradually, whereas the amount of perfectly rearranged lamellae increases. This explanation can be further supported by the fact that the total melting enthalpies of the sample keeps constant for different annealing time.

The previous experiment has demonstrated that annealing the sample at relatively large supercooling
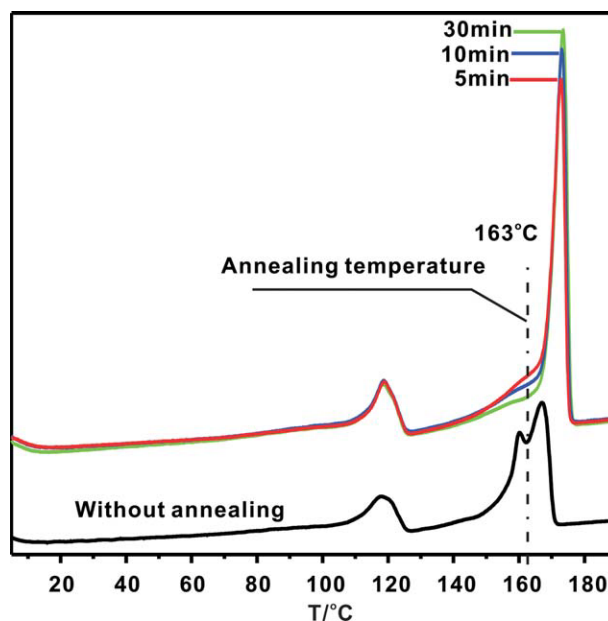

Figure 4 DSC endotherms of the PP in-reactor alloy annealed at 163°C for different time. The annealing time is indicated in the figure. An endotherm of the sample without annealing is also presented for comparison. [Color figure can be viewed in the online issue, which is available at wileyonlinelibrary.com.]
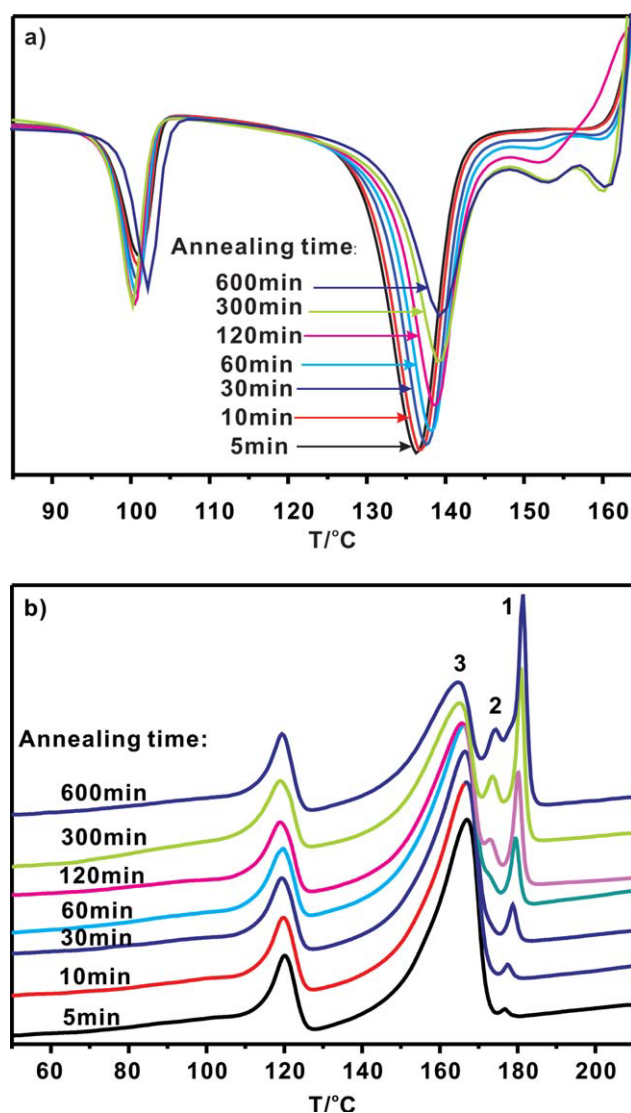
Figure 5 The DSC crystallization exotherms (a) and the subsequent melting endotherms (b) of the PP in-reactor alloy annealed at 167°C for different time. The annealing time is indicated above the corresponding curves in the figure. [Color figure can be viewed in the online issue, which is available at wileyonlinelibrary.com.]

(163°C) leads to a remarkable reduction of the imperfect lamellae and lamellae thickening. Annealing the sample at higher temperature in domain III, however, may lead to a significantly different melting behavior. Figure 5 shows the crystallization and the subsequent melting curves of the sample annealed at 167°C for different time. As shown in Figure 5(a), the crystallization peak of iPP shifts to higher temperature and the enthalpy decreases with increasing the annealing time. It is interesting to notice that two new exothermic peaks appear at much higher temperature range as the annealing time is longer than 30 min. The enthalpy of the higher crystallization peaks increases with annealing time. The multiple crystallization mechanism of the

PP component is still not well understood, however, it might be related to the nucleation effect of the annealed lamellae and the diffusion process of the melted PP molecules. Figure 5(b) shows the melting curve of the sample annealed for different time. Triple melting peaks were obtained by annealing the sample for more than 60 min. Peak 1 is assigned to the lamellae formed during the annealing process, which shifts to higher temperature with annealing time because of lamellae thickening. The presence of Peak 2 is quite surprising at first sight. However, it is understandable if we attribute it to the melting of the recrystallized lamellae during the heating process. With increasing annealing time, the more regular PP chains or segments diffuse to the surface of the crystalline phase formed in the temperature domain II and fold into the crystal lattice, and thus thicken the lamellae. Meanwhile, the defects in the crystal and the interphase are expelled into the amorphous phase as well, creating more chaos in the amorphous phase (or melting phase). So it is getting more difficult for the amorphous phase to form regular lamellae during the subsequent cooling scan, and thus incline to recrystallize during the heating scan. To summarize, Peak 1 is attributed to the primary crystallization during the annealing process, Peak 3 is attributed to the secondary crystallization during the cooling scan, and Peak 2 corresponding to the recrystallization in the heating process.

Nonisothermal crystallization and the subsequent melting behavior of PP in-reactor alloy

The multiple melting behavior of iPP has been a controversial topic among the authors for a long time. Recently, a consensus has been achieved gradually, considering it a result of recrystallization behavior during the heating process.[30–32] However, scarcely any direct evidence has been given. Figure 6 shows the endothermic traces of the alloy sample at different crystallization and melting rate. A typical bimodal lineshape can be observed for the sample experienced relatively high cooling rate and low heating rate. Detailed examination reveals that, generally, the intensity of the higher melting peak always decreases with increasing heating rate whereas increases with increasing cooling rate. For the quenched sample, no evidence of the lower melting peak was observed. This is because that no crystal was formed during the quench process. This explanation is strongly supported by the XRD data (Fig. 7), which shows that no diffraction peak from iPP was presented for the quenched sample. And the peak at 2θ degrees of 20° is assigned to the 111 planes of the orthorhombic form of polyethylene crystals. Based on the above observations, it is
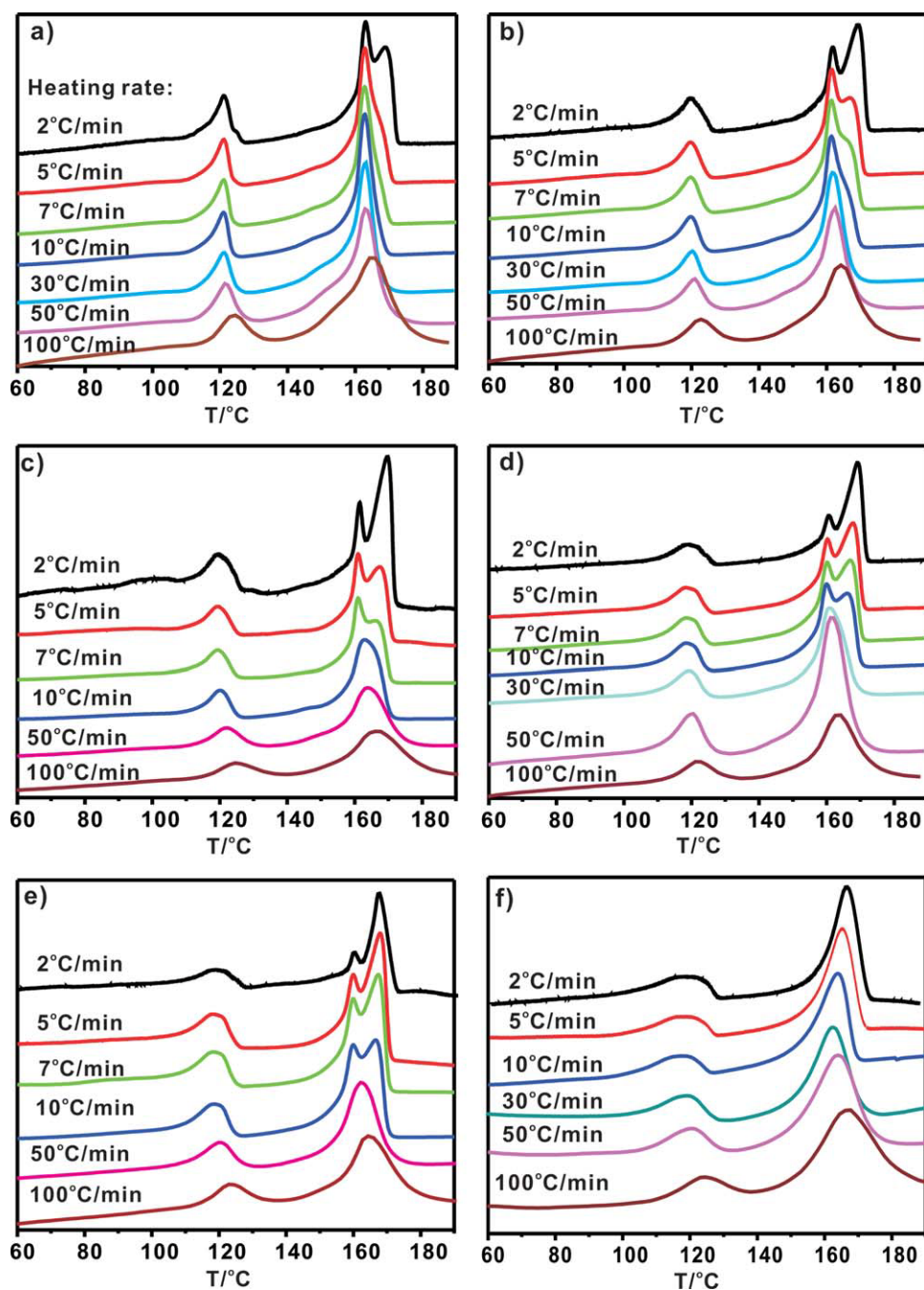
Figure 6 DSC melting endotherms of the PP in-reactor alloy nonisothermally crystallized under different cooling rate: (a) 2°C/min; (b) 7°C/min; (c) 10°C/min; (d) 30°C/min; (e) 50°C/min; (f) quenched in liquid nitrogen. The heating rates are indicated above the corresponding curves. [Color figure can be viewed in the online issue, which is available at wileyonlinelibrary.com.]

reasonable to infer that the lower melting peak is corresponding to the melting of the lamellae which were formed during cooling process; while the higher melting peak is ascribed to the melting of lamellae which were recrystallized during the heating process. In fact, there are three dynamic processes during the melting scan. Figure 8 shows the schematic illustration of the three dynamic processes. The primary and secondary lamellae of iPP,

which are also often referred to as mother and daughter lamellae, are displayed in Figure 8(a). In the first step of melting process, the defective secondary lamellae which are located among the primary lamellae melt, whereas leaving the primary lamellae intact. The second step is the recrystallization of the melted PP molecules in the first process. The unmelted lamellae act as hetero nucleus, and significantly reduce the crystallization energy barrier.
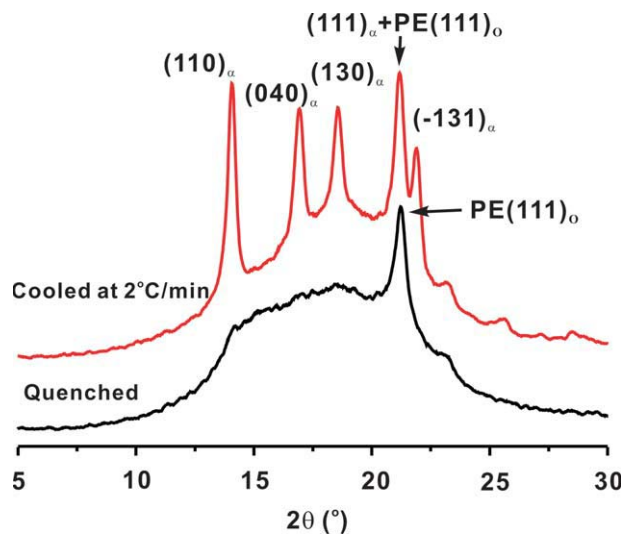
Figure 7 X-ray diffractograms of the slowly crystallized sample and quenched sample. The indexed peaks is assigned to the α-crystal form of iPP, whereas $PE(111)_o$ refers to the (111) planes of orthorhombic Polyethylene crystal form. [Color figure can be viewed in the online issue, which is available at wileyonlinelibrary.com.]

So the melted PP molecules can attach to the lamellae surface and thicken the unmelted lamellae. Actually, the first two dynamic processes (melting and recrystallization) happen almost at the same time and severely overlap with each other, as will be further discussed in the following text. On the other hand, however, the second step (recrystallization) is an exothermic process which can create minus signal on the endothermic curve, and thus can help to separate the two melting peaks. In the third process, the annealed and thickened lamellae melt at high temperature. In the case of quenched sample, however, only the last two process take place during the heating scan because no lamellae was formed originally. The amorphous or metastable phase recrystallizes into more stable crystalline phase and melts at higher temperature. So, a single melting peak at relatively high temperature was observed for the quenched sample.

It is notable that the melting peak of the quenched sample shifts to lower temperature as the heating rate increases. This may be explained by the fact that the recrystallization process is inhibited by the fast heating rate, and the PP molecules do not have enough time to arrange regularly into the crystalline phase due to its slow diffusion rate. So, the less perfect lamellae formed in the fast heating process are prone to melt at lower temperature. Actually, this result strongly supports our previous conclusion about the "three-step process" during the melting scan, because the melting temperature would not be affected by the heating rate if it were not the effect of the recrystallization process.
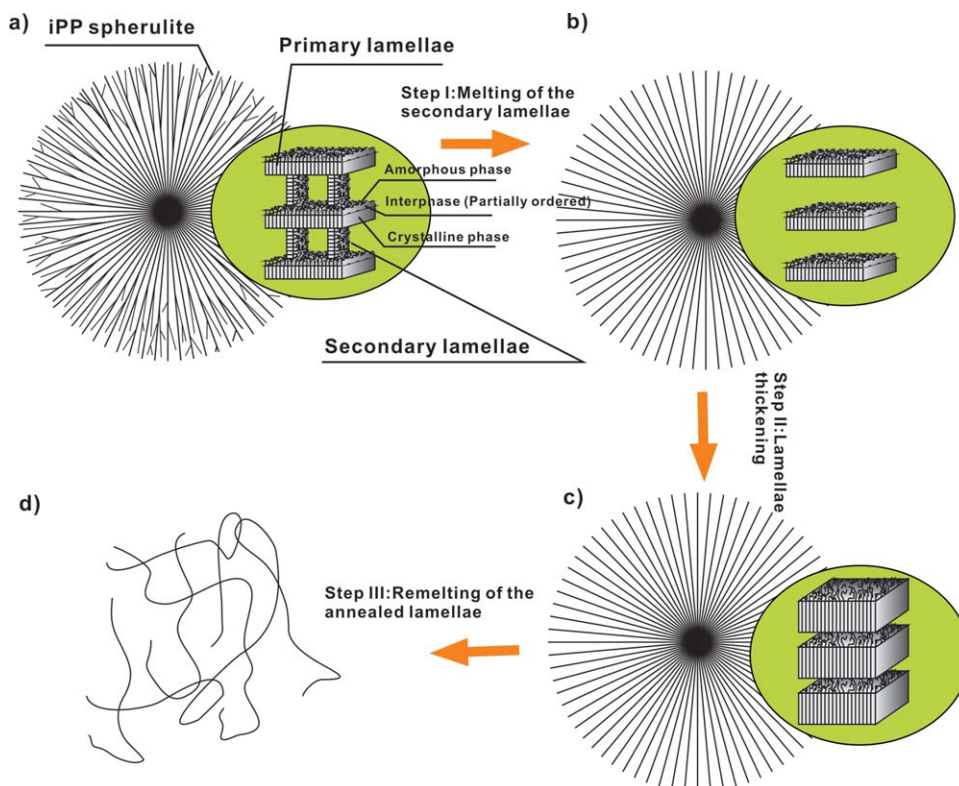

Figure 8 Schematic illustration of the melting and recrystallization processes of iPP in the in-reactor alloy during the heating scan. [Color figure can be viewed in the online issue, which is available at wileyonlinelibrary.com.]
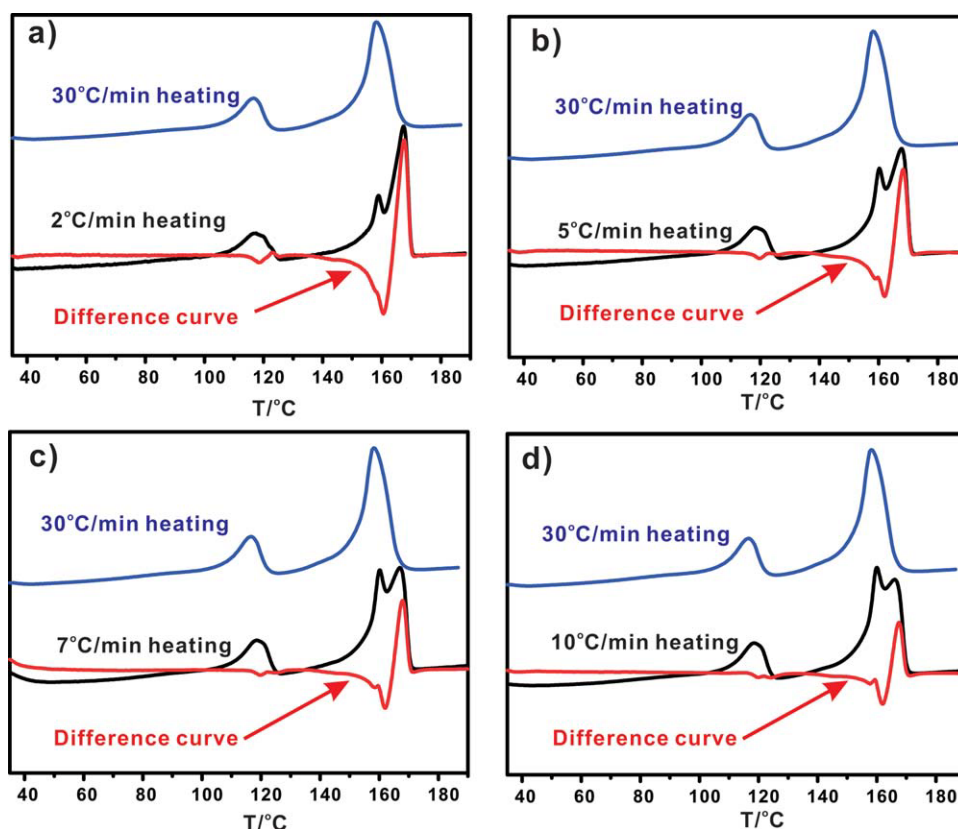
Figure 9 DSC melting endotherms of the PP in-reactor alloy crystallized at 10°C/min and their residual spectra. The heating rates of the corresponding thermograms are indicated in the figure. [Color figure can be viewed in the online issue, which is available at wileyonlinelibrary.com.]

Recrystallization is a dynamic process, usually existing in the melting process of polymers. Usually, the crystallization rate is controlled by diffusion process in the polymer melt system, because it generally takes long time for the macromolecules or the crystallizable chain segments to diffuse onto the surface of nuclei. If the heating rate is too fast, the molecules or the chain segments do not have enough time to diffuse to the boundaries of the crystalline region before melting, or they are too slow to rearrange into regular lamellae. So the recrystallization and the subsequent melting process will not occur under very fast heating rate. We assume that 30°C/min is fast enough to suppress the vast majority of recrystallization. If the fast melting curve is subtracted from the slow melting ones, one can directly see the recrystallization and the subsequent melting phenomenon from the residual spectra. Figure 9 shows the DSC melting curves of the sample crystallized at rate of 10°C/min and their difference curves. The intensities of all the thermograms were normalized for comparison. It can be seen that a "phase-twisted" peak is obtained in the difference curves. This can be explained by the overlapping of a downward peak and an upward peak. The downward peak is assigned to the recrystallization process, and the

upward peak is assigned to the melting of the recrystallized or annealed lamellae. It is also noted that the difference curves overlap very well with the original curve at high temperature end when the heating rate is low (e.g., 2°C/min), and the consistency loses with increasing heating rate. This is easily understood considering the fact that the recrystallization phenomenon is more prominent at lower heating rate, so the vast majority of the enthalpy of the high temperature peak comes from the melting of the recrystallized lamellae. As the heating rate increases, the contribution from the recrystallized lamellae reduces, and the melting enthalpy of the original lamellae which were formed during the cooling process dominates.

It is noticed that the recrystallization peak temperature is almost the same as the lower melting peak temperature, but slightly higher. This probably means that the recrystallization process happens immediately after the melting process. Recrystallization needs mobile molecules or segments as the material. However, mobile molecules are only available when the original crystals melt. The maximum quantity of crystallizable molecules and chain segments appear at the lower melting peak temperature and thus the recrystallization rate reaches maximum as well.
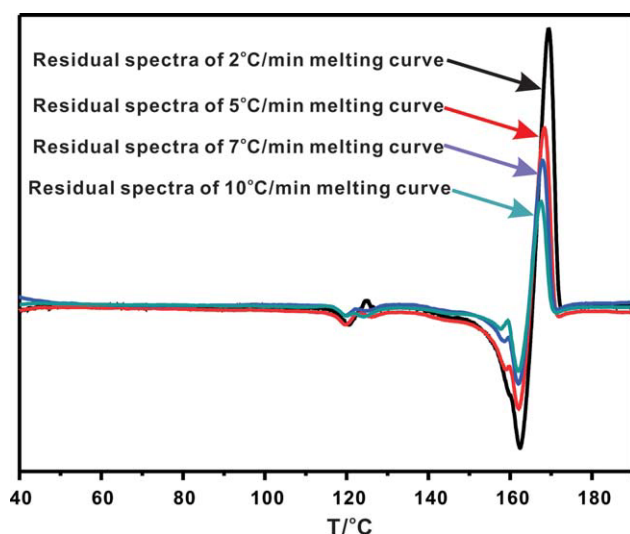
Figure 10 Stack plot of the residual spectra in Figure 7. [Color figure can be viewed in the online issue, which is available at wileyonlinelibrary.com.]

The residual spectra shown in Figure 9 were stack plotted in Figure 10 for comparison. The enthalpy of recrystallization and fusion decreases dramatically with increasing heating rate, and the melting temperature shifts to lower temperature, whereas the recrystallization peak temperature stays almost unchanged. This is because that the crystallizable molecules and chain segments have more time to diffuse to the edge of crystalline phase and to rearrange into thicker and more perfect lamellae when the heating rate is low. The peak temperature of recrystallization, however, is not dependent on the heating rate, but on the maximum quantity of crystallizable materials which is determined by the lower melting peak temperature.

Temperature modulated differential scanning calorimetry

TMDSC uses a periodic oscillation that is superimposed on a linear heating or cooling temperature program.[33] In addition to the total heat flow or heat capacity obtained from conventional DSC, an in-phase component, which is also referred to as reversing or storage heat capacity, is derived from the amplitude of the first harmonic of the Fourier transformation. It entails the heat effects associated with molecular changes that are reversing over the time and temperature of the modulation.[34,35] The nonreversing heat capacity represents the contribution to the heat flow that, at the time and temperature the measurement is made, is either irreversible or in some way kinetically hindered.[36] It can be determined from the difference between the total and reversing capacity. This simple analysis has been applied many times to many transitions, principally for polymer systems, and found to work well when the reversing

heat capacity is frequency-independent and the non-reversing process is the cold crystallization, chemical reaction, or the loss of volatile material.[37,38] The situation is somewhat more complex when considering glass transition because the reversing heat capacity is frequency dependent. When dealing with melting process, this analysis is not strictly valid, and the explanation of the nonreversing signal is not straightforward because the in-phase cyclic heat capacity does not depend solely on the reversing heat capacity as it derives from the latent heat of melting.

The melting endotherms presented in Figure 11 are the total, nonreversing and reversing specific heat curves obtained by TMDSC. The total specific heat curve shows multiple melting endotherms, with a similar profile to that obtained with linear heating at 2°C/min. The reversing specific heat curve shown in Figure 11 reveals that PP exhibits a reversible contribution during heating over the time and temperature of the measurement, with most occurring in the lower melting peak region of the total specific heat. A broad endotherm emerges with the peak temperature remaining at about 160°C (the same as the lower temperature peak of the total curve). This
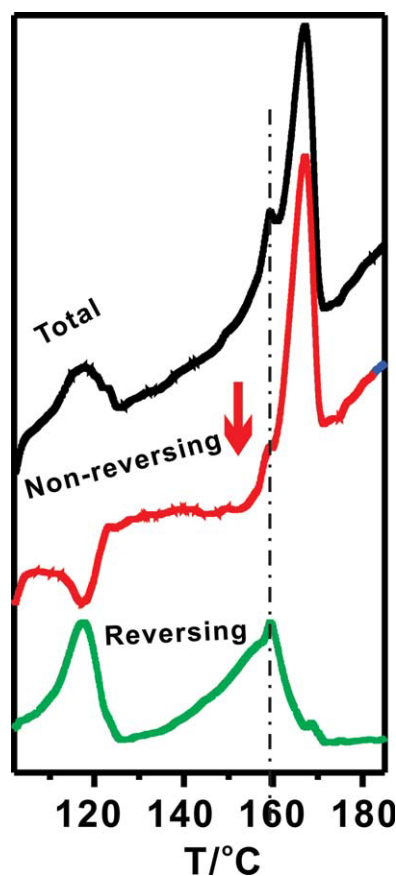

Figure 11 TMDSC specific heat melting curves of the PP in-reactor alloy after cooling linearly at the rate of 30°C/min. [Color figure can be viewed in the online issue, which is available at wileyonlinelibrary.com.]

means that the original melting process takes place very fast (without any kinetics involved), the imaginary part of the complex capacity is negligible and the real part is the static heat capacity plus the frequency independent part. Therefore, the melting of the original lamellae contributes primarily to the reversing signal. As the melting process proceeds, the melted chains or segments then can reattach to the same or an adjoining crystal surface with the exothermic energy released contributing to the cyclic signal. As more of the existing lamellae in the crystals thicken, the reversing contribution decreases. This is shown by the lower reversing contribution at higher temperature whereby most of the lamellae melt.

As has been demonstrated previously, the recrystallization proceeds quite rapidly even without localized cooling due to the already existed crystal surfaces which can act as a template. However, because the melting, recrystallization and remelting occur in the sample all while heating, the process may not be easily separated and therefore are partly obscured by competing events. The nonreversing specific heat curve in Figure 11 shows that the melting of the more ordered lamellae (higher temperature peak) is mostly irreversible at the temperature and time scale of the experiment. In contrast to the cold crystallization, the remelting process should take place not far from the equilibrium. This means that in the process of remelting, the entropy of the melt near the melting front is quite similar to the entropy of the crystal bulk. Therefore a relaxation of the entropy occurs. The reason for such a kinetics or time-dependence of the melting is local relaxation processes of the thermodynamic properties in the melt close to the crystal surface.

Before the main melting region of the curve, an obvious exothermic peak appears. This is due to the recrystallization process in the heating scan. The structure rearrangements that can occur during melting of the HPP component of the alloy involves an exothermic process, thus during the lower heating rate part of the cycle, exotherms occur that are balanced against melting endotherms during the higher heating rate segment of the modulation. This occurs as the dynamic equilibrium between the melt and crystalline phases oscillates back and forth. The result of this is that the in-phase heat capacity (reversing signal) appears very large, consequently the nonreversing signal appears exothermic. While this does not mean that there is a large net exotherm, it does indicate the presence of an exothermic process during the cycle. Because conventional DSC often shows very little when this kind of reorganization is taking place, this characteristic behavior of the nonreversing signal is useful indication that it is occurring.

CONCLUSIONS

Three annealing domains of the PP component in the PP in-reactor alloy were determined to be domain I (>171°C), domain II (171–168°C), and domain III (<168°C), respectively. The lowest temperature point in domain II (169°C) was chosen to be the first self-seeding temperature of the SSA experiment. The possible SSA fractionation mechanism of the sample was inferred. The first two melting peaks of the SSA curve are related to the recrystallization process during the heating scan rather than the molecular chain structure. The other melting peaks, however, are ascribed to the melting of the segmented E-P copolymers with different PP sequence lengths.

The melting of PP is a dynamic process which consists of three overlapping steps: melting, recrystallization, and remelting. By subtracting the fast-heating curve from the slow-heating one, the recrystallization and remelting processes have been observed directly. The temperature of melting of initial mesomorphic phase is found to be identical to the temperature of recrystallization or reorganization.

The multiple melting behaviors commonly observed for PP has been probed in the PP in-reactor alloy system by TMDSC. The less ordered lamellae of PP tend to reorganize to a larger degree than the more perfect lamellae, and in turn cause higher reversibility. The melting of the more ordered lamellae is mostly irreversible. The exothermic recrystallization process, which is normally obscured by the competing melting events, can be easily identified in the nonreversing specific heat curves.

References

1. Zheng, Q.; Shangguan, Y.; Yan, S.; Song, Y.; Peng, M.; Zhang, Q. Polymer 2005, 46, 3163.
2. Tan, H. S.; Li, L.; Chen, Z. N.; Song, Y. H.; Zheng, Q. Polymer 2005, 46, 3522.
3. Yamaguchi, M.; Miyata, H. Macromolecules 1999, 32, 5911.
4. Bartczak, Z.; Chiono, V.; Pracella, M. Polymer 2004, 45, 7549.
5. Galli, P.; Vecellio, G. Prog Polym Sci 2001, 26, 1287.
6. Fan, Z.; Zhang, Y.; Xu, J.; Wang, H.; Feng, L. Polymer 2001, 42, 5559.
7. Zhu, H.; Monrabal, B.; Han, C. C.; Wang, D. Macromolecules 2008, 41, 826.
8. Cui, N.; Ke, Y.; Lu, Z.; Wu, C.; Hu, Y. J Appl Polym Sci 2006, 100, 4804.
9. Pires, M.; Mauler, R. S.; Liberman, S. A. J Appl Polym Sci 2004, 92, 2155.
10. Fu, Z.; Fan, Z.; Zhang, Y.; Xu, J. Polym Int 2004, 53, 1169.
11. Zacur, R.; Goizueta, G.; Capiati, N. Polym Eng Sci 1999, 39, 921.
12. Xu, J.; Feng, L. Polym Int 1998, 47, 433.
13. Tselios, C.; Bikiaris, D.; Maslis, V.; Panayiotou, C. Polymer 1998, 39, 6807.
14. Zhu, X.; Li, Y.; Yan, D.; Fang, Y. Polymer 2001, 42, 9217.
15. Zhu, X.; Yan, D.; Tan, S.; Wang, T.; Yan, D.; Zhou, E. J Appl Polym Sci 2000, 77, 163.
16. Al-Raheil, I. A.; Qudah, A. M.; Al-Share, M. J Appl Polym Sci 1998, 67, 1267.

17. Janimak, J. J.; Cheng, S. Z. D.; Giusti, P. A.; Hsieh, E. T. Macromolecules 1991, 24, 2253.
18. Kamide, K.; Yamaguchi, K. Die Makromol Chem 1972, 162, 219.
19. Kawai, T. Die Makromol Chem 1965, 84, 290.
20. Mezghani, K.; Anderson Campbell, R.; Phillips, P. J. Macromolecules 1994, 27, 997.
21. Kim, Y. C.; Ahn, W.; Kim, C. Y. Polym Eng Sci 1997, 37, 1003.
22. Al-Raheil, I. A.; Qudah, A. M.; Al-Share, M. J Appl Polym Sci 1998, 67, 1259.
23. Zia, Q.; Androsch, R.; Radusch, H. J.; Piccarolo, S. Polymer 2006, 47, 8163.
24. Lorenzo, A. T.; Arnal, M. L.; Mueller, A. J.; de Fierro, A. B.; Abetz, V. Macromol Chem Phys 2006, 207, 39.
25. Müller, A. J.; Arnal, M. L. Prog Polym Sci 2005, 30, 559.
26. Pijpers, M. F. J.; Mathot, V. B. F.; Goderis, B.; Scherrenberg, R. L.; van der Vegte, E. W. Macromolecules 2002, 35, 3601.
27. Fillon, B.; Wittmann, J. C.; Lotz, B.; Thierry, A. J Polym Sci Part B: Polym Phys 1993, 31, 1383.
28. Arnal, M. L.; Sánchez, J. J.; Muller, A. J. SPE ANTEC 99, Conference Proceedings, 1999, 2329.
29. Müller, A. J.; Hernandez, Z. H.; Arnal, M. L.; Sánchez, A. J Polym Bull 1997, 39, 465.
30. Liu, T. Eur Polym J 2003, 39, 1311.
31. De Rosa, C.; Guerra, G.; Napolitano, R.; Petraccone, V.; Pirozzi, B. Eur Polym J 1984, 20, 937.
32. Cox, W. W.; Duswalt, A. A. Polym Eng Sci 1967, 7, 309.
33. Paukkeri, R.; Lehtinen, A. Polymer 1993, 34, 4083.
34. Swier, S.; Van Assche, G.; Van Hemelrijck, A.; Rahier, H.; Verdonck, E.; Van Mele, B. J Therm Anal Calorimetry 1998, 54, 585.
35. Gill, P. S.; Sauerbrunn, S. R.; Reading, M. J Therm Anal 1993, 40, 931.
36. Jones, K. J.; Kinshott, I.; Reading, M.; Lacey, A. A.; Nikolopoulos, C.; Pollock, H. M. Thermochim Acta 1997, 304–305, 187.
37. Schawe, J. E. K.; Bergmann, E. Thermochim Acta 1997, 304–305, 179.
38. DaSilva, A. L. N.; Tavares, M. I. B.; Politano, D. P.; Coutinho, F. M. B.; Rocha, M. C. G. J Appl Polym Sci 1997, 66, 2005.